

# Mechanisms for Crystal Phase Transformations by Heat Treatment and Molecular Motion in Poly(vinylidene fluoride)

Yasuhiro Takahashi,\* Yoshiaki Matsubara, and Hiroyuki Tadokoro

Department of Macromolecular Science, Faculty of Science, Osaka University, Toyonaka, Osaka 560, Japan. Received April 23, 1981

**ABSTRACT:** Mechanisms for crystal phase transformations caused by heat treatment in poly(vinylidene fluoride) are interpreted mainly in terms of cooperative motions around single bonds in a molecule. Two modes of motion, the segmental flip-flop motion and the inversion motion, are associated with the transformation from form II to form III. The segmental flip-flop motion, which begins to occur at about 150 °C, gradually changes the molecular conformation from  $(TGT\bar{G})_n$  to  $(T_3GT_3\bar{G})_n$ . The inversion motion, which begins to occur at about 170 °C, changes the molecular packing from the antiparallel structure to the parallel structure. Furthermore, the transformation from form IIp to form III caused by heat treatment and the transformation from form II to form I caused by high-pressure heat treatment are discussed on the basis of molecular motion.

Poly(vinylidene fluoride) has been found to exist in four crystal forms, I,<sup>1</sup> II,<sup>1</sup> III,<sup>2</sup> and polar II (IIp).<sup>3-6</sup> Many researchers have reported that transformations among the four crystal forms take place under various conditions such as heat treatment, stretching, and poling. Heat treatment causes transformations from form II to form III<sup>7-9</sup> and from form IIp to form III<sup>10</sup> under atmospheric pressure and transformations from form II to form I, from form II to form III, and from form III to form I under high pressure.<sup>11-15</sup> The transformation from form II to form III has so far only been studied in the unoriented state. In previous papers,<sup>3,16,17</sup> we found that the transformation from form II to form III can take place in an oriented state, via streak II. Streak II is named for form II, which shows X-ray diffuse streak scatterings on the fiber diagram and which is characterized as an intermediate phase between forms II and III. We have clarified the structure and formation mechanism of streak II as well as the crystal structures of forms II<sup>1</sup> and III.<sup>2</sup>

In the present study, a mechanism is proposed for the transformation from form II to form III from a viewpoint of molecular motion. Mechanisms are also discussed for transformations caused by high-pressure heat treatment and for the transformation from form IIp to form III.

## Experimental Section

X-ray diffraction measurements were made by using Cu K $\alpha$  radiation monochromatized by a graphite crystal. Fiber photographs were taken by cylindrical cameras of 4.5- and 5.0-cm radii in a stream of He gas.

The poly(vinylidene fluoride) sample used for this study was KF1100 (Kureha Chemical Industry Co., Ltd.). A uniaxially oriented sample of form II was prepared by crystallizing the melt by elongation at room temperature. This sample was clamped in a metal holder and heat treated. After heat treatment at 150 °C for 24 h, X-ray diffuse streak scatterings (streaks) appeared on the lines of constant  $\xi$  from Bragg reflections on the fiber diagram (Figure 1b).<sup>16,17</sup> The resulting fiber specimen of streak II was successively annealed for 24 h at 165, 170, 175, and 180 °C. The fiber diagram of the sample before heat treatment is shown in Figure 1a and fiber diagrams after annealing at 150, 170, and 180 °C are shown in Figure 1b-d, respectively. Streak II almost completely transforms to form III during annealing at 175 °C for more than 10 days.<sup>2</sup> On the other hand, in a conventionally prepared fiber specimen of form II which was prepared by stretching the unoriented form II at about 150 °C in an oil bath, only a trace of form III was found after annealing at 180 °C for more than 10 days.

Servet and Rault<sup>10</sup> reported that form IIp transforms into a new form in which the molecule may assume a  $T_3GT_3\bar{G}$  conformation during heat treatment at 170 °C. In the present study, this form was characterized as form III on the basis of its fiber diagram, although Lovinger<sup>18,19</sup> suggested the possibility that this

form may be an antipolar analogue ( $\epsilon$  phase) of form III. The transformation was found to occur even at 150 °C. Here, an oriented film of form IIp was prepared by corona poling of an oriented film of form II which was made by stretching unoriented form II at about 150 °C.

Phase transformations caused by heat treatment in poly(vinylidene fluoride) are summarized in Figure 2.

## Transformation from Form II to Form III

**Crystal Structures of Forms II and III.** The crystal structures of forms II<sup>1</sup> and III<sup>2</sup> are shown in Figure 3. In form II, two molecular chains in the  $(TGT\bar{G})_n$  conformation are contained in a rectangular unit cell with parameters  $a = 4.96$  Å,  $b = 9.64$  Å, and  $c$  (fiber axis) = 4.62 Å and monoclinic space group  $P2_1/c-C_{2h}^5$ . In form III, two molecules in the  $(T_3GT_3\bar{G})_n$  conformation are contained in a monoclinic unit cell with parameters  $a = 4.96$  Å,  $b = 9.58$  Å,  $c$  (fiber axis) = 9.23 Å, and  $\beta = 92.9^\circ$  and space group  $Cc-C_s^4$ . Recently, Lando et al.<sup>6,20,21</sup> reported that form II belongs to the orthorhombic system (space group  $P2cm$ ) and is statistically disordered so that up- and down-pointing molecules occupy the same site in the unit cell with equal probabilities. However, the tilting sample clearly shows that form II belongs to the monoclinic system. Furthermore, a reexamination of the structure shows that the regular structure shown in Figure 3 is essential although it contains some kind of disorder. A detailed structural analysis will be published in the near future. The crystal structure of form III was briefly reported in a previous paper.<sup>2</sup> However, Weinhold et al.<sup>22</sup> independently reported an orthorhombic structure (space group  $C2cm$ ) for form III, in which up- and down-pointing molecules occupy the same site in the unit cell with equal probabilities. Recently, Lovinger<sup>18,19</sup> supported our monoclinic unit cell for form III by electron diffraction measurements. The details of the structural analysis will be published soon in an article that will clearly distinguish the structure from the model of Weinhold et al.

The  $a$  and  $b$  values of form III are very similar to those of form II and moreover, the angle  $\beta$  of form III is close to a right angle, i.e.,  $\beta$  of form II. The  $c$  value of form III is twice as long as that of form II. In form II, two molecules in the unit cell are related by the center of symmetry and hence they differ in orientation. In form III, two molecules are related only by simple translation and have the same orientation. Accordingly, during the transformation from form II to form III, the molecular conformation changes from  $(TGT\bar{G})_n$  to  $(T_3GT_3\bar{G})_n$  and the  $c$  value is doubled. As for the molecular packing, one of two molecular chains changes its orientation so that two molecules pack parallel to each other.

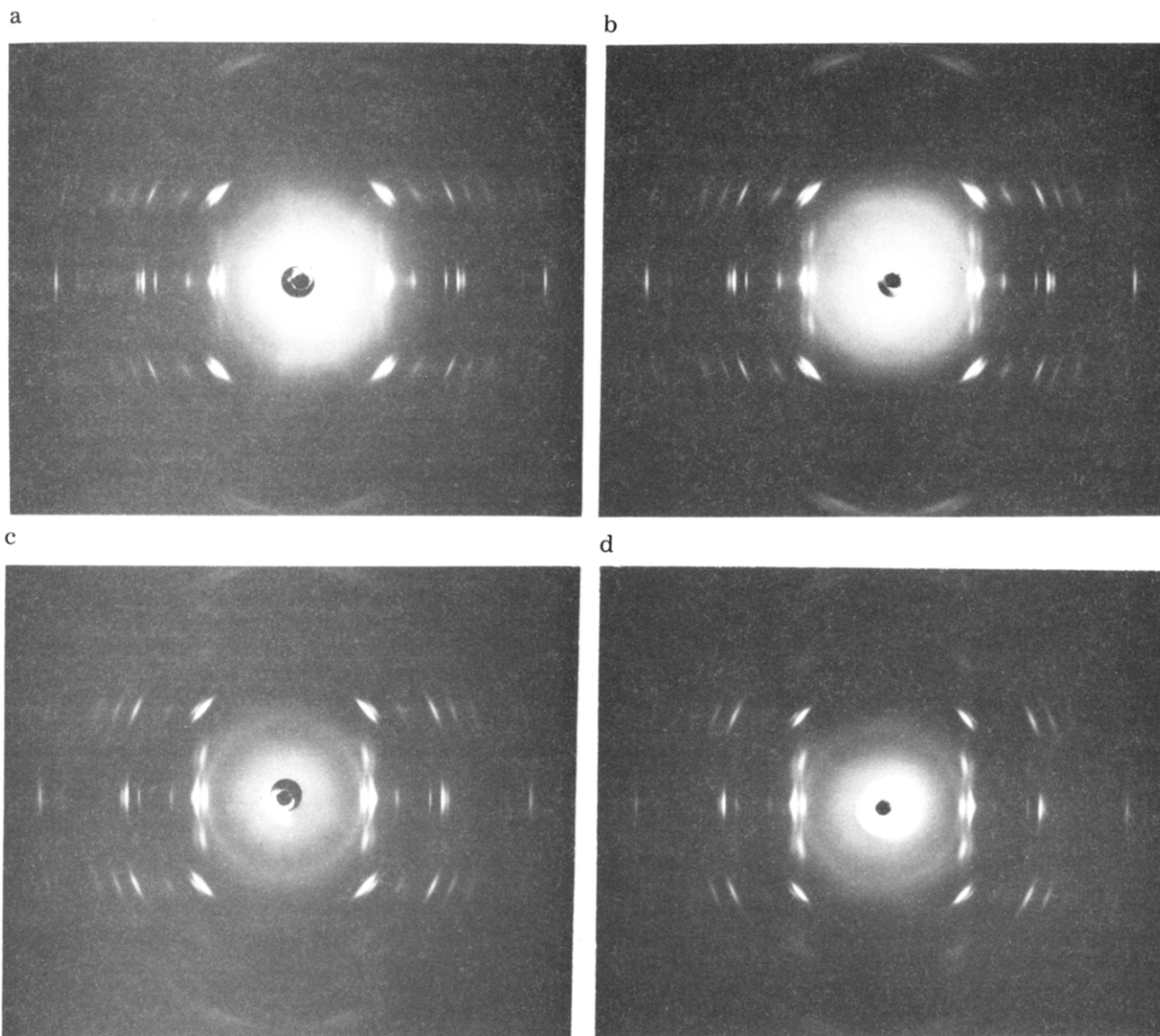


**Figure 1.** (a) Fiber diagram of the sample prepared by stretching and crystallizing the melt at room temperature. Fiber diagrams after annealing at (b) 150, (c) 170, and (d) 180 °C in successive heat treatments at 150, 165, 170, 175, and 180 °C for 24 h each.

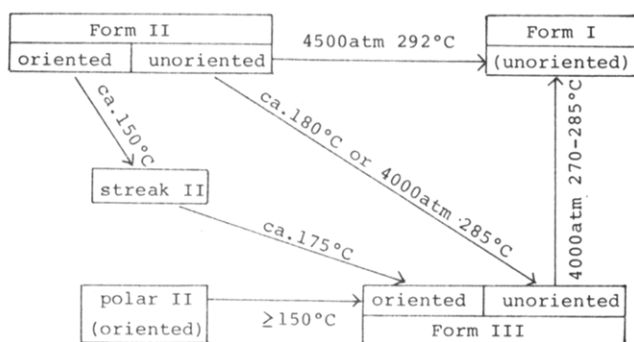


**Figure 2.** Crystal phase transformations caused by heat treatment in poly(vinylidene fluoride).

### Structure and Formation Mechanism of Streak II.

The structure and formation mechanism of streak II, which is characterized as an intermediate phase between forms II and III, have been briefly reported in previous papers.<sup>16,17</sup> X-ray diffuse streak scatterings observed on the fiber diagram of streak II are attributed to kink bands contained in the crystallite (Figure 4), in which the molecule assumes the TT conformation. The kink band is one monomeric unit thick and the size on the plane perpen-

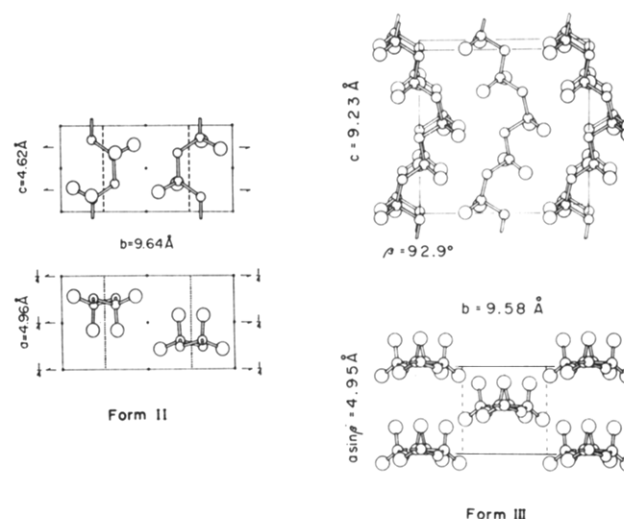


**Figure 3.** Crystal structures of forms II and III.

dicular to the fiber axis is considered to be a little smaller than that of the crystallite since the width of the streak is slightly broader than that of the Bragg reflection. In a segment of the molecule in the (TGTG)<sub>n</sub> conformation,

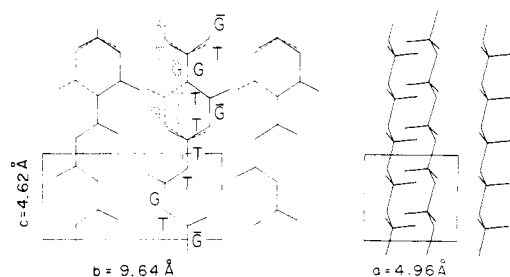


Figure 4. Kink band contained in streak II.

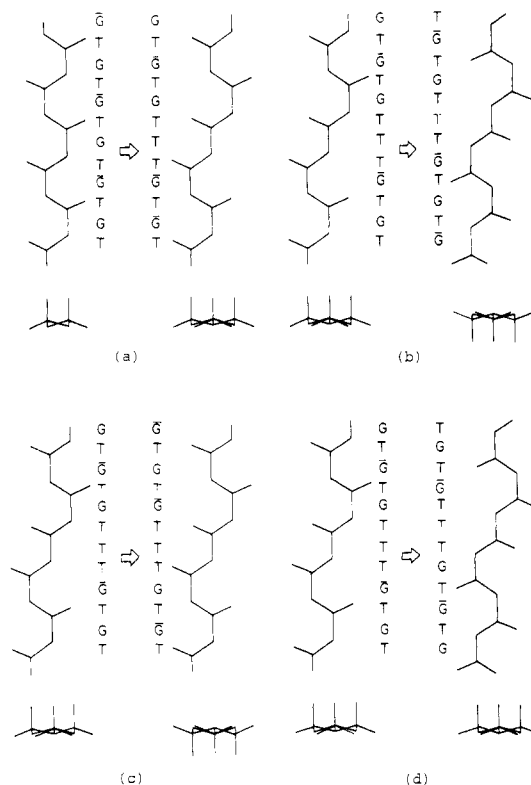


Figure 5. Four modes of molecular motion which may be associated with the phase transformations: (a) segmental flip-flop motion, which occurs between G and  $\bar{G}$  and which introduces a TT conformation; (b) inversion motion, which reverses the molecular orientation both on the  $c$  projection and along the chain axis; (c) and (d) motion that reverse the molecular orientation on the  $c$  projection and along the chain axis, respectively.

a flip-flop motion between G and  $\bar{G}$  occurs during heat treatment and a TT conformation is introduced as a joint between the segment in which the motion occurred and the segment in which the motion did not occur. Hereafter, this motion is designated as the segmental flip-flop motion.

**Mechanism for Transformation from Form II to Form III.** Four modes of motion, which may be associated with the transformation, are shown in Figure 5. The motion shown in Figure 5a is the segmental flip-flop motion, which is similar to the so-called crankshaft motion. Repetition of the motion brings about a conformational change from  $(TGT\bar{G})_n$  to  $(T_3GT_3\bar{G})_n$  by successive introduction of TT conformations.<sup>2</sup> Lovinger<sup>9</sup> independently proposed that this type of motion takes part in the transformation. The following three modes of motion result in an orientational change of the molecule. The motion shown in Figure 5b, by which G and  $\bar{G}$  change to T, and T changes to G or  $\bar{G}$ , results in the reverse of the molecule both on the  $c$  projection and along the chain axis. This motion is designated as the inversion motion hereafter. The motion shown in Figure 5c, which changes G

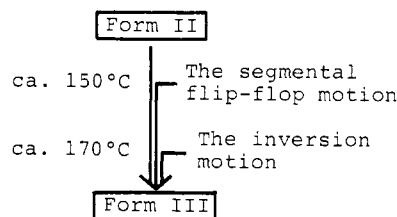
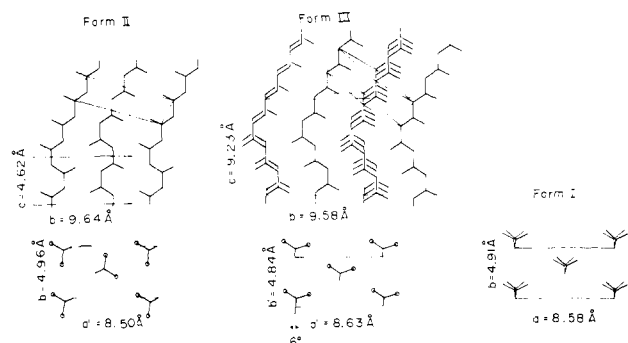


Figure 6. Schematic representation of the transformation from form II to form III.

to  $\bar{G}$ , and  $\bar{G}$  to G over a whole molecule, reverses the molecule only on the  $c$  projection, which corresponds to  $180^\circ$  rotation about the chain axis. This motion was proposed to take part in the transformation from form II to form IIp and from form II to form III by Lovinger.<sup>18,19,23</sup> The motion shown in Figure 5d, by which G and  $\bar{G}$  change to T, and T changes to G or  $\bar{G}$ , is similar to the inversion motion but it changes only the chain direction. The packing change during the transformation from form II to form III could be explained in two ways: one is the inversion motion and the other is the combination of the motions shown in (c) and (d) of Figure 5. In either case, during the transformation, the motions take place cooperatively among the molecules in a crystallite.

The structural change during the transformation from form II to form III could be read on the X-ray fiber diagram after the heat treatments (Figure 1). As seen in Figure 1a, very weak streaks are observed on the fiber diagram of the original sample before the heat treatment. After heat treatment at  $150^\circ\text{C}$  for 24 h, the intensities of the streaks become very strong. Here, the concentration of the kink band is considered to reach an equilibrium state (streak II). Hereafter, the streaks become sharper with increasing temperature of heat treatment and finally, after heat treatment at  $180^\circ\text{C}$ , the streaks are almost Laue spots. Little intensity change is observed on the Bragg reflections at heat treatments below  $170^\circ\text{C}$ . Thereafter, the intensities of the Bragg reflections gradually change with increasing temperature and almost coincide with those of form III after the heat treatment at  $180^\circ\text{C}$ . Their location on the fiber diagram is virtually unchanged during the heat treatment. The change in the fiber diagram is described by two processes: one is the appearance of the streaks and their transformation to the spots, and the other is the intensity change on the Bragg reflections. The former process corresponds to the conformational change from  $(TGT\bar{G})_n$  to  $(T_3GT_3\bar{G})_n$  caused by the segmental flip-flop motion (Figure 5a) and the latter process corresponds to the packing change from the antiparallel structure to the parallel structure. For the latter process, two mechanisms could be considered as mentioned already. One is the inversion motion (Figure 5b) and the other consists of two modes of motion (Figure 5c,d). If the latter process involves two modes of motion, it could be further divided into two processes because it must pass over not only two energy barriers corresponding to the transition states of two modes of motion but also the energy minimum, which has almost the same value as it has in the two states before and after the process. In fact, the latter process is considered to be a single process, since the intensities of the Bragg reflections monotonically change and a new X-ray diffuse streak scattering does not appear. Accordingly, it is likely that the packing change is caused only by the inversion motion. Furthermore, the inversion motion is considered to take place cooperatively and almost simultaneously in a molecule. The mechanism for the transformation from form II to form III is schematically shown in Figure 6. The inversion motion results in the



**Figure 7.** Structures of a kink band assumed in form II and a kink band assumed in form III, and the structure of form I on the *c* projection.

**Table I**  
Unit Cell Parameters of Form I and Assumed Values for Kink Bands in Forms II and III

	form I	kink band in form II	kink band in form III
<i>a</i> , Å	8.58	8.72	8.65
<i>b</i> , Å	4.91	4.96	4.84
<i>c</i> , Å	2.56	2.62	2.56 <sup>a</sup>
$\alpha$ , deg	90	90	92
$\beta$ , deg	90	103	94
$\gamma$ , deg	90	90	90
$\theta$ , deg <sup>b</sup>	$\pm 7$	65, -115	6

<sup>a</sup> This value was assumed. <sup>b</sup> Angle between molecular plane and *bc* plane.

reverse of the chain direction, which also results from the motion proposed by Miyamoto et al.<sup>24</sup> They explained the anisotropy of the  $\alpha$  relaxation of form II by a motion which reverses the chain direction through the movement of a defect region in a molecule. However, with an inversion motion, it is not necessary to consider that a defect region plays any role in reversing the molecule in form II.

### Transformations by High-Pressure Heat Treatment

Form II transforms into form I under high-pressure heat treatment (4500 atm, 292 °C), and form II transforms into form III at 285 °C and form III transforms into form I at 280 °C under 4000 atm (Figure 2). The transformation from form II into form III under high pressure is considered to occur by the same mechanism as that under atmospheric pressure.

In the transformations from form II into form I and from form III into form I, the molecular conformations,  $(TGT\bar{G})_n$  and  $(T_3GT_3\bar{G})_n$ , change to the planar-zigzag conformation in form I. These conformational changes are considered to be caused by the formation of the kink band and its growth in thickness resulting from the repetition of the segmental flip-flop motion (Figure 5a). The structure in the kink bands of forms II and III with a thickness of several monomeric units is shown in Figure 7 together with the structure of form I. The unit cell parameters assumed for the kink bands in forms II and III are listed in Table I together with those of form I. Packing of the planar-zigzag molecules in the kink band of form III is very similar to that of form I, but the molecular packing in the kink band of form II is different from that of form I. Accordingly, in the transformation from form III to form I, the molecular conformation  $(T_3GT_3\bar{G})_n$  first changes to the planar-zigzag structure by the segmental flip-flop motion, and a slight displacement of the molecule to the stable position results in form I. The transformation from form III to form I is caused almost

entirely by the segmental flip-flop motion.

On the other hand, two mechanisms can be considered for the transformation from form II into form I. The first mechanism is rather similar to that for the transformation from form III into form I as mentioned above. After the molecular conformation  $(TGT\bar{G})_n$  changes to the planar-zigzag structure by the segmental flip-flop motion, a fairly large displacement of the molecule results in the transformation into form I. The second mechanism is similar to that for the transformation from form II into form III. The conformational change by the segmental flip-flop motion and the packing change by the inversion motion proceed simultaneously. In other words, form II transforms into form I via form III or a structure close to form III with respect to the molecular packing. The large rotation of the planar-zigzag molecule about the molecular axis is proposed for the poling process of form I,<sup>25,26</sup> but this is not necessarily the case for the heat treatment. From analogy with the transformation from form II into form III, the latter mechanism is considered to be more probable. The crystalline densities of three crystal forms (form II, 1.93 g/cm<sup>3</sup>; form III, 1.94 g/cm<sup>3</sup>; form I, 1.97 g/cm<sup>3</sup>), which may indicate their stability under high pressure, may support the latter mechanism.

### Transformation from Form Iip into Form III

Form II transforms into form Iip by poling, and form Iip easily transforms into form III by heat treatment (Figure 2). In form Iip, the cell parameters are the same as those of form II and the molecule assumes the same  $(TGT\bar{G})_n$  conformation as in form II. On the *c* projection, two molecules in the unit cell assume the same orientation in contrast with form II. However, three kinds of models differing in chain direction have been proposed so far: the parallel model,<sup>3</sup> the antiparallel model,<sup>4,5</sup> and the statistically disordered model.<sup>6</sup> The conformational change in the transformation from form Iip into form III is considered to be caused by repetition of the segmental flip-flop motion. The packing change occurs by different mechanisms, depending upon the models for form Iip. In the parallel model, two molecules in the unit cell have the same direction. Therefore, in the transformation from form II into form Iip by poling, the molecular orientation changes both on the *c* projection and along the chain axis, which corresponds to the inversion motion, and form Iip transforms into form III only by the segmental flip-flop motion. In the antiparallel model, two molecules in the unit cell are different in the chain direction. The poling process reverses the molecule only on the *c* projection, which corresponds to the motion shown in Figure 5c, and form Iip transforms into form III by two modes of motions, the segmental flip-flop motion and the motion shown in Figure 5d. In the statistically disordered model, up- and down-pointing molecules occupy the same site in the unit cell with equal probabilities. Here, the poling causes the orientational change corresponding partly to the inversion motion and partly to the motion shown in Figure 5c, and form Iip transforms into form III partly by the segmental flip-flop motion and partly by combining with the motion shown in Figure 5d. Form Iip transforms into form III at 150 °C (Figure 2), which corresponds to the temperature at the outset of the segmental flip-flop motion in the transformation from form II into form III. This may suggest the possibility that form Iip transforms into form III only by the segmental flip-flop motion and hence form Iip is the parallel structure.

**Acknowledgment.** This work was partially supported by a Grant-in-Aid for Scientific Research from the Min-

istry of Education, Japan (Grant No. 555354).

## References and Notes

- (1) Hasegawa, R.; Takahashi, Y.; Chatani, Y.; Tadokoro, H. *Polym. J.* **1972**, *3*, 600.
- (2) Takahashi, Y.; Tadokoro, H. *Macromolecules* **1980**, *13*, 1317.
- (3) Davis, G. T.; McKinney, J. E.; Broadhurst, M. G.; Roth, S. C. *J. Appl. Phys.* **1978**, *49*, 4998.
- (4) Naegle, D.; Yoon, D. Y.; Broadhurst, M. G. *Macromolecules* **1978**, *11*, 1297.
- (5) Davies, G. R.; Singh, H. *Polymer* **1979**, *20*, 772.
- (6) Bachman, M.; Gordon, W. L.; Weinhold, S.; Lando, J. B. *J. Appl. Phys.* **1980**, *51*, 5095.
- (7) Osaki, S.; Ishida, I. *J. Polym. Sci., Polym. Phys. Ed.* **1975**, *13*, 1071.
- (8) Lovinger, A. J.; Keith, H. D. *Macromolecules* **1979**, *12*, 919.
- (9) Lovinger, A. J. *Polymer* **1980**, *21*, 1317.
- (10) Servet, B.; Rault, J. *J. Phys. (Paris)* **1979**, *40*, 1145.
- (11) Hasegawa, R.; Kobayashi, M.; Tadokoro, H. *Polym. J.* **1972**, *3*, 591.
- (12) Doll, W. W.; Lando, J. B. *J. Macromol. Sci., Phys.* **1968**, *B2*, 219.
- (13) Doll, W. W.; Lando, J. B. *J. Macromol. Sci., Phys.* **1970**, *B4*, 889.
- (14) Doll, W. W.; Lando, J. B. *J. Macromol. Sci., Phys.* **1970**, *B4*, 897.
- (15) Matsushige, K.; Takemura, T. *J. Polym. Sci., Polym. Phys. Ed.* **1978**, *16*, 921.
- (16) Takahashi, Y.; Kohyama, M.; Tadokoro, H. *Macromolecules* **1976**, *9*, 870.
- (17) Takahashi, Y.; Tadokoro, H. *Macromolecules* **1980**, *13*, 1316.
- (18) Lovinger, A. J., private communications.
- (19) Lovinger, A. J. *Macromolecules* **1981**, *14*, 322.
- (20) Lando, J. B., private communications.
- (21) Bachmann, M. A.; Lando, J. B. *Macromolecules* **1981**, *14*, 40.
- (22) Weinhold, S.; Litt, M. H.; Lando, J. B. *Macromolecules* **1980**, *13*, 1178.
- (23) Lovinger, A. J. *Macromolecules* **1981**, *14*, 227.
- (24) Miyamoto, Y.; Miyaji, H.; Asai, K. *J. Polym. Sci., Polym. Phys. Ed.* **1980**, *18*, 597.
- (25) Kepler, R. G.; Anderson, R. A. *J. Appl. Phys.* **1978**, *43*, 1232.
- (26) Takahashi, N.; Odajima, A. *Rep. Prog. Polym. Phys. Jpn.* **1978**, *21*, 141.

## Molecular Weight Dependence of the Noncrystalline Component in Dilute-Solution-Grown *trans*-1,4-Polybutadiene Crystals

Susan Tseng, William Herman,<sup>†</sup> and Arthur E. Woodward\*

Department of Chemistry, The City University of New York, City College, New York, New York 10031

Brian A. Newman

Department of Mechanics and Materials Science, Rutgers University, Piscataway, New Jersey 08854. Received July 6, 1981

**ABSTRACT:** Eight *trans*-1,4-polybutadiene preparations were obtained by crystallization from dilute heptane and, in one case, toluene solutions. The crystal preparations, as characterized by gel permeation chromatography, had  $\bar{M}_n$  values of 4700 to  $1.2 \times 10^5$  and  $\bar{M}_w/\bar{M}_n$  values of 1.3 to 2.7. Mats of these crystals were investigated by differential scanning calorimetry, density measurements in a gradient column, low-angle X-ray diffraction and/or electron microscopy, and reaction at the crystal surfaces with *m*-chloroperbenzoic acid in toluene. The heat of transition from DSC was found to be proportional to the specific volume. The number of monomer units per fold,  $U$ , and the number per chain end,  $C/2$ , were obtained from an equation that relates these two parameters to the crystal thickness,  $L_c$ , the fraction of double bonds at the crystal surfaces, the repeat distance along the polymer chain, and  $\bar{M}_n$ . Assuming  $U$  to be constant and  $C$  to be a function of the lamellar thickness,  $L$ , values of 3.8 monomer units per fold and  $0.79L/2R$  units per chain end were obtained. Assuming  $C$  to remain at  $0.79L/R$  and allowing  $U$  to vary yield values that show a decrease occurring with decreasing crystallization temperature.

## Introduction

In earlier reports<sup>1-4</sup> investigations of the noncrystalline component at the surfaces of solution-grown *trans*-1,4-polybutadiene, TPBD, lamellas using epoxidation, bromination, and broad-line NMR in the presence of a nonprotonated liquid were described. Some evidence was given to suggest that the surface component is composed of two parts, one due to the chain folds and the other to the chain ends or cilia, the latter component becoming of greater importance at lower molecular weights. Calculation of the average number of monomer units per fold from the values for the surface component and the lamellar thickness yielded values of 2.5-5.5 for the three preparations studied.<sup>4,5</sup> In this earlier work infrared spectroscopy<sup>2</sup> and differential scanning calorimetry<sup>6</sup> were used to estimate the total noncrystalline content in order to determine the presence of any material within the crystals that was not available to determination by surface techniques.

<sup>†</sup> Undergraduate research participant supported through the National Science Foundation Undergraduate Research Participation Program.

Table I  
Characteristics of TPBD Samples

sample	polymer prep conditions	$\bar{M}_n \times 10^{-4}$	$\bar{M}_w/\bar{M}_n$
W	urea canal complex	7.9	3.5
V		2.2	2.5
U	RhCl <sub>3</sub> -sodium alkylbenzenesulfonate	0.70	3.0

The purpose of the current study was to investigate the noncrystalline component in TPBD lamellas over a wider molecular weight range (4700 to  $1.2 \times 10^5$ ) than that previously covered, using the epoxidation method to evaluate the surface fraction and density measurements to evaluate the total noncrystalline content. In this investigation molecular weight fractions with  $\bar{M}_w/\bar{M}_n = 1.3-2.7$  are used. Differential scanning calorimetry measurements in the regions of the crystal-crystal transition and the melting transition were also made for each sample to determine the usefulness of  $\Delta H_{Tr}$  and/or  $\Delta H_m$  in assessing the total noncrystalline fraction. A method of analysis of the epoxidation results was developed to enable determination of the number of monomer units per fold